-RESEARCH PAPER-

International Journal of Mining and Geo-Engineering

IJMGE

IJMGE 57-4 (2023) 455-460

DOI: 10.22059/IJMGE.2023.366283.595102

Spatially weighted singularity mapping in conjunction with random forest algorithm for mineral prospectivity modeling

Saeid Ghasemzadeh [a, b *], Abbas Maghsoudi [a], Mahyar Yousefi [c], Oliver P. Kreuzer [d, e]

[a] Department of Mining Engineering, Amirkabir University of Technology, Tehran, Iran.

[b] Iranian Mines and Mining Industries Development and Renovation Organization (IMIDRO).

[c] Faculty of Engineering, Malayer University, Malayer, Iran.

[d] Corporate Geoscience Group, PO Box 5128, Rockingham Beach, WA 6969, Australia.

[e] Economic Geology Research Centre, College of Science & Engineering, James Cook University, Townsville, QLD 4811, Australia.

Article History:

Received: 05 October 2023.

Revised: 27 October 2023.

Accepted: 19 November 2023.

ABSTRACT

Geochemical exploration data play a vital role in mineral prospectivity modelling (MPM) for discovering unknown mineral deposits. In this study, the improved spatially weighted singularity mapping (SWSM) method is used to improve the practice of identifying geochemical anomalies related to copper mineralization in the Sarduiyeh district, Iran. Then, the random forest algorithm (RF) and geometric average function (GA) are used to integrate the resulting geochemical predictor map with other predictor maps. As demonstrated by the high area under the curve (AUC) values, this approach can effectively delineate prospective areas with RF and GA. However, compared to the GA approach (AUC=0.78), the RF technique (AUC = 0.98) offers superior prediction capabilities due to its enhanced ability to capture spatial correlations between predictive maps and known mineral deposits. The proposed procedure, a hybrid of the improved SWSM and RF has outstanding predictive capabilities for identifying prospective areas. A case in point is the new, highly prospective areas identified in this study, which present priority targets for future exploration in the Sarduiyeh district.

Keywords: *Anisotropic singularity; Geochemical signature; Mineral prospectivity modelling; Sarduiyeh.*

1. Introduction

GIS-based mineral prospectivity modelling (MPM) is a multi-step process that employs powerful mathematical algorithms to produce a predictive model (e.g., [1-21]). Generally, these steps include (i) defining a conceptual model for mineral deposits of the type of interest, (ii) collecting geoscience spatial datasets, (iii) enhancing and extracting evidential features, (iv) generation weighted evidence layers and (v) generating a predictive model (e.g., [4-5], [7], [12], [22]). Hence, MPM is a highly complex decision-making task in mineral exploration targeting [20]. To implement an effective MPM, it is necessary to consider various aspects that may affect its results [2], [22-29]. The robustness of the underlying conceptual targeting model, the quality of multi-source and multi-scale exploration data, and predictive ability of the generated evidence layer have a substantial impact on the effectiveness of this modelling (e.g., [16], [28], [30]). Thus, a better understanding of ore-forming geological processes [15], [27], [31]and improved analysis of exploration data are required to make MPM more geologically meaningful [32-33]. In regional-scale mineral exploration, geochemical evidence layers are a vital input for MPM [22], [33-37]. Such predictor maps capture geochemical anomalies likely caused by a mineralizing system. As such, they present mappable evidence in support of the likely presence of a mineral deposit and an efficient parameter for delineating exploration target areas [30], [38- 42]. Therefore, capturing an efficient multi-element geochemical signature for use in MPM is a critical task [19], [28], [33], [43]. In this regard, to answer the question "how to generate a comprehensive geochemical signature that is statistically valid, geologically meaningful, and practically useful?" Ghasemzadeh et al. [28] (2022) proposed a strengthened singularity mapping technique ([44-46]) that was spatially enhanced and weighted by mineralization-efficient fault systems, which act as pathways or traps[47-48] .They proved that an improved spatially weighted method of mapping anisotropic geochemical signature (i.e., singularity), through the application of distance-distribution analysis[49] on fault systems and the RF integration approach (RF; [50]), is a more effective technique compared to the existing spatially weighted principal component analysis, to model geochemical anomalies. Following Ghasemzadeh et al. [28], this paper focuses on integrating SWSM-based enhanced geochemical signature with other evidential maps representing a set of targeting criteria using two high-performance modelling techniques to identify highly prospective areas for the sought deposit-type in the Sarduiyeh area in support of mineral exploration.

2. Study area and Dataset

In this paper, the Sarduiyeh district, which is located in the Kerman province, Iran is used as the study area. This region, as a part of the

* Corresponding author. *Tel:* +98 9105877442, *E-mail address:* Ghasemzadeh.saeid.ge@gmail.com (S. Ghasemzadeh).

Urumieh-Dokhtar magmatic belt (Fig.1a), is considered to have excellent potential for Cu mineral exploration, especially porphyry copper system exploration, as several moderate to large porphyry-Cu deposits (PCDs), including Bondar Hanza, Daralu, and Sarmeshk have been found in this study area (e.g., [51, 52]). In addition, this area is highly prospective for other types of deposits such as Fe, Zn, and Pb [53]. The lithological units outcropping in the area are Cretaceous mélanges, Eocene volcanic rocks, sedimentary rocks of Eocene age, intrusive rocks, Oligocene–Miocene sediments, Neogene volcanic rocks, and Quaternary alluvial deposits (Fig.1b) [53]. The volcanic rocks of Eocene age (pyroclastics, trachyandesites, trachybasalts, andesite-basalts, andesite lavas, tuffaceous sediments, rhyolites, rhyolite tuffs, agglomerate tuffs, agglomerates, ignimbrites, basaltic rocks and andesites) are intruded by Cretaceous, Eocene, Oligocene–Miocene and Neogene granodiorites, quartz-diorites, diorites, diorite porphyry, granite-porphyry and granites [53]. The area has undergone multiple stages of tectonic deformation, resulting in fault and fold systems [51-53]. Ore minerals in the porphyry-Cu deposits are mainly galena, sphalerite, chalcopyrite, bornite, pyrit, and magnetite, while gangue minerals are mainly diopside, chlorite, epidote, quartz, calcite, and apatite [51-53]. Lineaments and faults in the study area were also specified using topography and geology maps of the Sarduieh and ASTER data. There are 23 known porphyry copper deposits (Fig.1b).

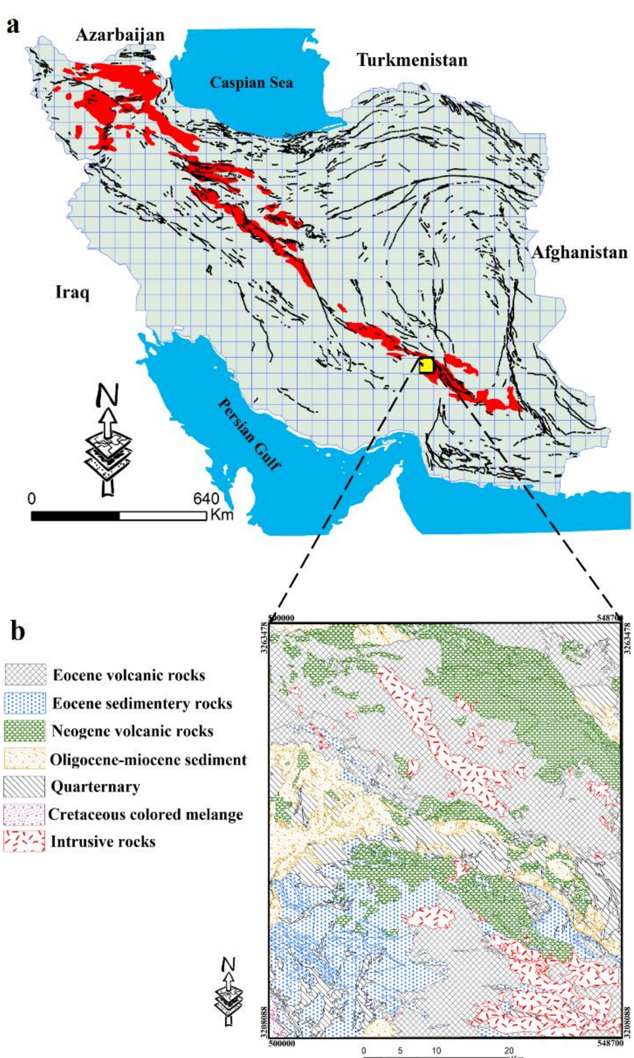

Fig.1. (a) Location of the study area in Urumieh-Dokhtar volcanic belt of Iran and (b) simplified geological map of the study area.

For a geochemical survey, the generation of a geochemical dataset is essential. The main sequential steps adopted in this study were: (i) sampling and (ii) analysis. In the first stage, 893 stream sediment samples were collected with a sampling density of one sample per km2. In this stage, the type of deposit sought, the tectonic setting of the study area, and the geological unit age are considered. In the second stage, the collected samples were air dried, sieved at 80 mesh, and analyzed for 15 elements (i.e., Cu, Ag, As, Sb, Zn, Pb, Bi, Co, Cd, Cr, Ni, Mn (by Atomic Absorption Spectroscopy (AAS)), W, Mo (by Polarography) and Au (by Atomic Emission Spectroscopy (AES)). Among the analyzed elements, the concentration values of Cu, Mo, Au, Ag, As, Sb, Zn, and Pb are used in the current study to illustrate the implementation of the methods proposed in this paper. Frequency distributions of all measured elemental data are positively skewed, indicating that the original data are not normally distributed (e.g., [54]).

3. Methods and results

3.1. Generation of evidence layers from exploration criteria

According to the conceptual model of the porphyry-Cu deposit, different evidential layers can be derived from different types of individual mineral exploration datasets (e.g., geochemical data, geological data, multi-spectral remote sensing data, etc.). In this regard, a general flow chart that illustrates the study steps is summarized in Fig. 2. Map visualization and spatial representation were processed using ArcGIS.10.7 software. The singularity mapping technique and machine learning algorithms have been coded and implemented in MATLAB R2016a workspace and R statistical freeware, respectively. Also, Microsoft Excel 2016 and Envi5.1 have been used as helpful software for mapping some plots and processing remote sensing data, respectively.

In regional-scale exploration, the spatial distributions of ore-forming elements in stream sediment have been routinely used to prospect porphyry-Cu deposits [30], [33], [38], [40]. In this study, we used stream sediment uni-element concentration data of Cu, Mo, Au, Ag, As, Sb, Zn, and Pb to generate a multi-element geochemical signature for MPM. For modelling mineralization-related geochemical anomalies in the study area, concentration values of the indicator elements as mentioned above, were processed by an improved spatially weighted singularity mapping technique [28]. In terms of multi-fractal modelling, the SWSM model can be summarized as follows[45]: Assuming that ξ (ds) is the total amount of element concentration from samples in a small sampling domain of ds and w (ds) ($0 \le w(ds) \le 1$) indicates the corresponding weighting factor that represents the importance of the samples in ds, the singularity phenomenon in two-dimensional space can be described as a power law relationship between spatially weighted area $S_i = \iint_0^{S_i} w\,(ds)ds$ and spatially weighted areal concentration $\varphi(S_i) = \iint_0^{S_i} w(ds).\,\xi\,(ds)ds$:

$$\varphi(S_i) = S_i^{\epsilon/2} \quad (1)$$

where the symbol ∝ stands for proportionally, and the exponent ϵ is the anisotropic singularity index.

Processing of the geochemical exploration data by the improved SWSM technique, compared to using original raw data, not only allows for better discrimination of geochemical anomalies but also improves the prediction-rate of mineral occurrences in the MPM [28], [46]. Then, calculated anisotropic singularity value of indicator elements (i.e., Cu, Mo, Au, Ag, As, Sb, Zn, and Pb) were combined using a random forest algorithm (Breiman, 2001) to generate a more robust multi-element geochemical signature of porphyry-Cu mineralization in the study area (Fig. 3a).

Porphyry-Cu deposits are mostly spatially and genetically associated with intrusive rocks, including felsic to intermediate porphyritic [55]. The prominent role of these intrusions in the form of mineralization is that they are the most apparent geological expression that acts as a heat engine, facilitating and marking the fluid flux [16], [20], [22], [27], [31],

[56]. Hence, the mineralization is expected to occur in the proximity of intrusive contacts, with the likelihood of a deposit being present decreasing with the increasing distance (e.g., [57]). Hence, in this study, to represent that empiricism and to create a fuzzy map of proximity to intrusive contacts (Fig.3b), Euclidian distance from intrusive contacts was calculated and fuzzified using Eq. [2].

$$F_x = \frac{1}{1+e^{-s(x-i)}} \tag{2}$$

Where F_x is the fuzzy score, i and s are the inflexion point and slope, respectively, of the logistic function, and x is a raster map to be transformed in the [0,1] range. In the Eq [2], i and s can be calculated by $i = \frac{EV_{max}+Ev_{min}}{2}$ and $s = \frac{9.2}{EV_{max}-Ev_{min}}$; where EV_{max} and EV_{min} are maximum and minimum value in an input raster evidence layer (e.g., [57]). Therefore, Fig.3b indicates that the greatest distances from the intrusive contacts are assigned the lowest fuzzy scores, in contrast, the smallest distances from the intrusive contacts are assigned the highest fuzzy scores.

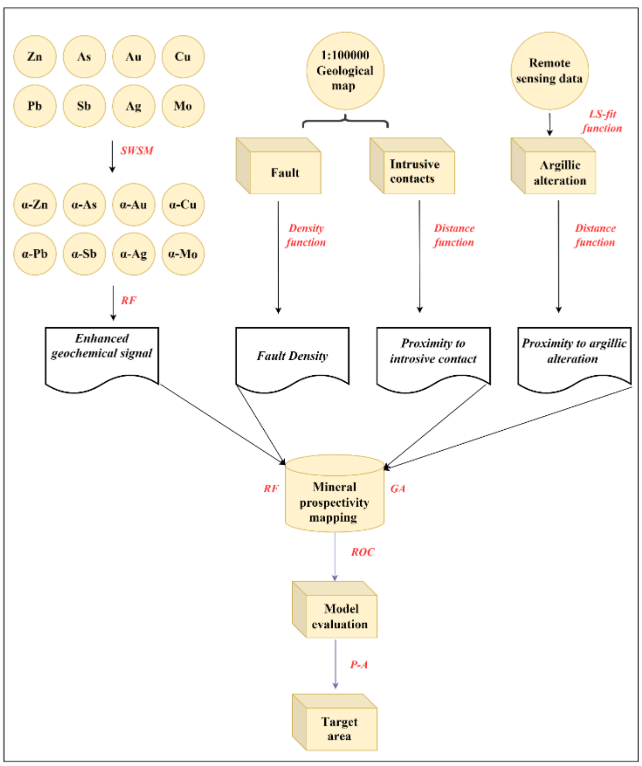

Fig.2. Flow chart for illustrating the steps of procedures in this study.

In the study area, different types of faults affected the lithological units. These fault zones act as primary channel ways for deeply sourced melts and facilitate the migration of ore-bearing fluid [15-16], [27], [58-59]. Thus, areas with high fault density (FD) represent favorability for porphyry-Cu mineralization. In this paper, we used FD as an evidence layer (to represent structural control evidence of prospectivity for porphyry-Cu mineralization) in the study area. Then, for transforming the FD values into logistic space, we applied Eq. [2] to obtain a weighted evidence map of FD (Fig. 3c).

Porphyry-Cu deposits are associated with various hydrothermal alteration types ([60], some of which, such as argillic alteration, extend a few to tens of kilometers around mineralization trap sites (e.g., [55], [61]). Thus, these wall-rock alterations are important targeting criteria for prospecting porphyry-Cu deposits. In this study, argillic alteration areas have been recognized from ASTER data using the LS-fit function. Then, to generate proximity to argillic alteration, we applied the Euclidian distance function around centroids of these proxies and weighted them using a logistic-based continuous approach (i.e., Eq [2]). The Map of proximity to argillic alteration is shown in Fig. 3d.

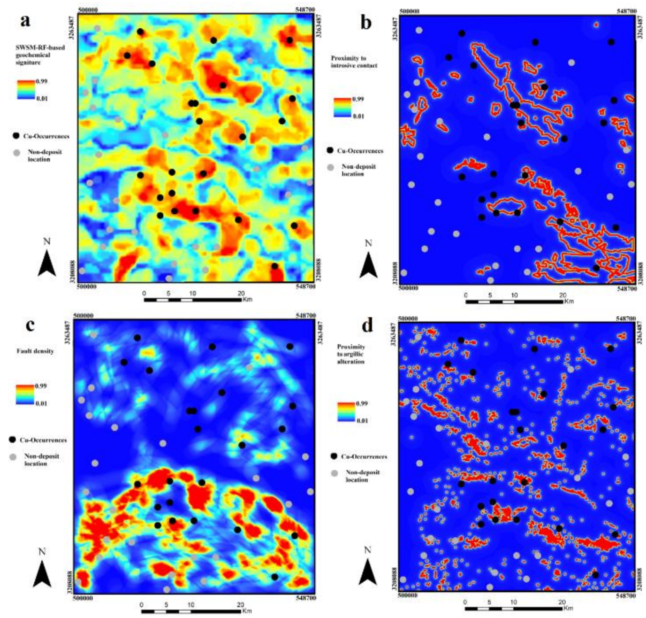

Fig.3. Derived evidence layer fromm exploration data (a) SWSM-based multi-element geochemical signiture (b) proximity to intrusive contacts (c) fault density (d) proximity to argilic alteration.

3.2. Integration of generated evidence maps for mineral exploration targeting

It is generally accepted that each evidence layer contains information about how mineralization is formed by representing a particular mappable criterion [3], [27], [58]. Thus, after the generation of various evidence layers, they should be integrated based on measured spatial or genetic associations with the targeted mineral deposits and each other [27], [62-66]. For this, numerous researchers have proposed and applied various methods, which are classified into two groups, including data-driven and Knowledge-drive to integrate multiple evidential layers for the MPM to delineate target areas for further exploration of a certain deposit-type (e.g., Porphyry Cu-deposit) [2], [7-9]. In this paper, to integrate the generated evidential layer, we applied two different functions, namelythe geometric average [9] function and the random forest algorithm [50], [62-63], [67] for comparison purpose.

The geometric average (GA; [9]) is an unsupervised integration function without using training data. This GIS base integrates the values of various evidence maps in a single but comprehensive model. The main advantage of the GA method is that it integrates both optimistic and pessimistic input evidence layers to produce an effective and comprehensive MPM model. Hence, according to the proposed equation by Yousefi and Carranza [9], to generate a porphyry-Cu exploration targeting model in a unit cell of a study area, GA can be defined as the n^{th} root of the products of input indicator values as follows:

$$G_{A_{Porphyry-Cu}} = (F_{FD}, F_{IC}, F_{GS}, F_{FA}) =$$

$$(\prod_{i=1}^{4} F_i)^{0.25} = \sqrt[4]{F_{FD}, F_{IC}, F_{GS}, F_{FA}} \tag{3}$$

where F_{FD}, F_{IC}, F_{GS}, and F_{FA} denote, respectively, maps of fault density, proximity to intrusive contacts, SWSM-based multi-element geochemical signature, and proximity to argillic alteration. The GA-based prospectivity model for porphyry-Cu deposit using Eq [3] is shown in Fig.4a.

The RF algorithm ([50]), is a supervised and data-driven integration method. RF ([50]) is one of the well- regarded ensemble models, which can be used efficiently for the MPM [62-63]. RF is known as a homogeneous ensemble model, because it uses a collection of a single base learning algorithm ([68], [69]), DTs, to predict a target variable based on evidential variables [6], [62-63], [67]. These DTs can be categorized into classification and regression trees (RTs) [50]). For the MPM, the RF is based on the regression mode of DT [70]. In this study, we generated a RF-based prospectivity model using the same four spatial evidence layers for comparison with the GA-based prospectivity model (Fig.4b).

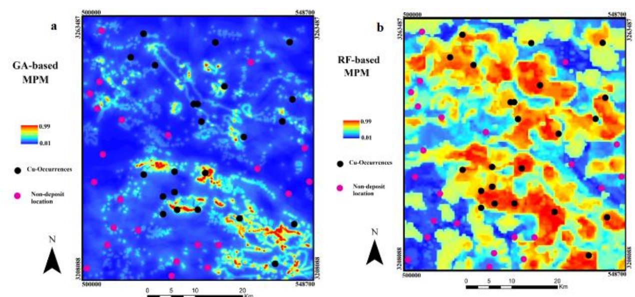

Fig.4. Prospectivity map for porphyry-Cu deposits generated through integrating multiple evidence layers using (a) Geometric average function (b) random forest algorithm.

4. Evaluation of the model

Evaluation of mineral prospectivity model results and measuring the success of exploration targeting is an absolutely essential task [71-73]. In this paper, the receiver operating characteristic curve (ROC) ([72], [74-75]) was employed to evaluate the efficiency of the prospectivity models generated by GA and RF. The ROC curve for both prospectivity models (Fig. 5) appears above the gauge line. The results of high AUC values indicate that implemented modelling can effectively delineate prospective areas both with RF and GA; however, compared with the GA (with AUC=0.78), the RF performs better prediction capabilities (with AUC=0.98) due to its enhanced ability to capture the correlations between predictive maps and known mineral deposits. The continuous prospectivity score, is generated using the RF algorithm, as an efficient model, should be discretized to delimit exploration targets. In this study, therefore, the prediction-area (P-A; [8]) plot (Fig. 6a) was used as a quantitative criterion to delimit target areas for further exploration (e.g., [33]). As recommended by Yousefi and Carranza [8], the X value corresponding to the intersection point in the P-A plot (Fig.6a) was conducted to determine the reliable threshold for classification. Thus, 0.9 was extracted as the threshold for making highly favorable delineated exploration targets (Fig.6b).

5. Discussion

Mineral exploration is a multi-stage activity that seeks to progressively reduce prospective areas and refine drill targets until a discovery is made. The MPM is most useful in the initial stages of mineral exploration and at scales ranging from regional to camp scale [15], [76-77]. For the MPM of a certain deposit type (e.g., porphyry deposits) within a particular target area, a set of multi-disciplinary data has to be compiled, collated, and analyzed effectively (e.g., [27], [77]). Despite the development of various simple to complex mathematical methods over the past decades, the MPM continues to be a challenging task (e.g., [25]). For example, the application of incorrect or inappropriate modelling approaches can not only heighten exploratory bias and uncertainty but also lead to failure arising from missed opportunity costs linked to spending time and money on exploring and testing unprospective targets [59], [78]. As discussed by Yousefi et al. [27], Zuo and Xiong [37], and Zuo [79], extracting information from mineral exploration data (e.g., geochemical data), generating knowledge

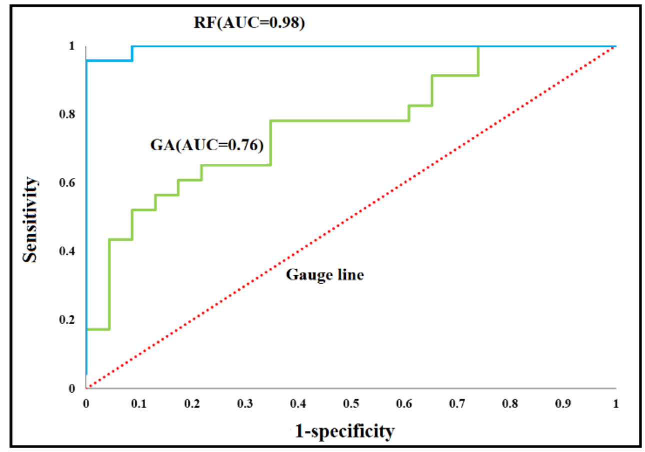

Fig.5. ROC plots for the evaluation capabilities of random forest algorithm and geometric average function for mineral prospectivity modeling.

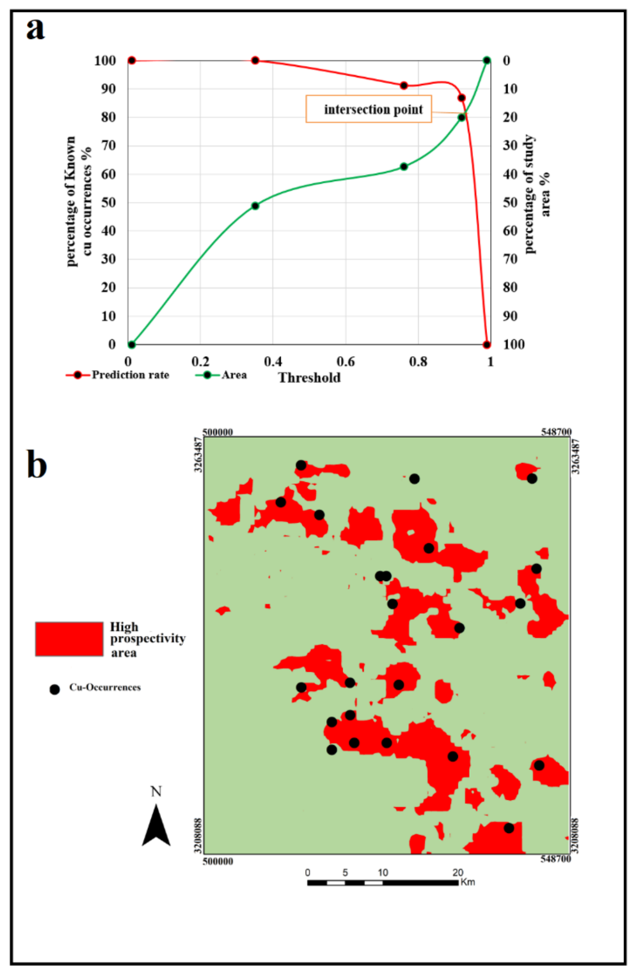

Fig.6. (a)P-A plot for RF-mineral prospectivity model (b) Highly favorable delineated exploration targets for porphury-Cu deposits in Sarduiyeh district.

from this information, and gaining insight from this knowledge are appropriates solution for defining more reliable mineral exploration targets.

In this regard, stream sediment samples are representative of the lithologies exposed to erosion upstream [19], [28], [35], [40], [42], [44], [80-82]. Thus, such surface media, as weathered derivatives of rocks, are essential sources of information. Consequently, processing of stream sediment geochemical data and the methods of anomaly pattern recognition are effective ways to gain geological knowledge, giving the exploration geologists insights to recognize better and more effectively follow up any anomalous results [27], [36-37]. Thus, to obtain insights into the definition of exploration strategies aimed at vectoring toward undiscovered mineral deposit sites, it is critical to develop innovative techniques for extraction of mineralization-associated anomalies from stream sediment geochemical data [83-84]. The improved SWSM technique ([28]), which has the ability of recognizing mineralization-related geochemical anomalies, was used to map anisotropic singularity values of elements, indicating the presence of mineral deposits in this study.

Geochemical indicator elements show dispersion halos in and around mineral deposits in response to some ore-forming factors such as magma composition, the reaction between hydrothermal fluids and wall rocks, and/or sulfur species gradient in ore-bearing hydrothermal fluids [85-86]. Therefore, dispersion halos of every indicator element contain helpful information about the ore-deposition processes, which should be routinely extracted from the geochemical data [27], [36], [43]. Consequently, integrating the geochemical indicators results in a more robust signature, helping exploration geologists to vector towards undiscovered deposit sites. In this study, to generate an upgraded geochemical signature (Fig.3a), the RF algorithm ([50]) was applied.

For the evaluation of mineral exploration targeting models, which were generated using GA and RF integration methods, we applied the ROC curve (Fig.5) [72], [74-75]. A Comparison of the integration results demonstrated that the RF is superior to GA for targeting areas with potential for porphyry-Cu deposits. It is important to note here that, RF unlike non-parametric supervised classifiers known as single classifiers, such as support vector machines [5], [87], deliver excellent results in the field of MPM. This is because the RF algorithm is not sensitive to the quality of training samples and overfitting.

6. Conclusion

In this paper, a case study applies the improved Spatially Weighted Singularity Mapping (SWSM) technique for identifying geochemical anomalies associated with porphyry-Cu mineralization in the Sarduiyeh district. Then, the SWSM-based multi-element geochemical signature was integrated with other evidential layers for Mineral Prospectivity Modelling (MPM) to delineate target areas for further exploration using both random forest (RF) algorithm and Geometric average (GA) method.

The findings of this study can be summarized as follows:

- The improved SWSM can simultaneously model element enrichment and depletion, consequently, it can be used to derive a more robust geochemical signature for use in the MPM.
- The improved SWSM not only facilitates a better understanding of ore-forming geological processes but also improves the prediction-rate of the MPM.
- The hybrid approach used here, which combines the improved SWSM, RF, and prediction-area plot, is an effective tool for delineating target areas.

Acknowledgments

The authors would like to sincerely thank Dr. Maysam Abedi for expertly handling this paper and the two anonymous reviewers whose comments and suggestions helped significantly improve the quality of this contribution.

REFERENCES

[1] Bonham-Carter, G.F., 1994. Geographic Information Systems for Geoscientists: Modelling With GIS. Pergamon, Oxford.

[2] Carranza, E. J. M. 2008. Geochemical anomaly and mineral prospectivity mapping in GIS. Elsevier.

[3] Porwal, A., Gonz´alez-´Alvarez, I., Markwitz, V., McCuaig, T.C., Mamuse, A., 2010. Weights-of-evidence and logistic regression modeling of magmatic nickel sulfide prospectivity in the Yilgarn Craton, Western Australia. Ore Geol. Rev. 38, 184–196.

[4] Porwal, A.K., Kreuzer, O.P., 2010. Introduction to the special issue: mineral prospectivity analysis and quantitative resource estimation. Ore Geol. Rev. 38, 121–127.

[5] Abedi, M., Norouzi, G.H., Bahroudi, A., 2012. Support vector machine for multi-classification of mineral prospectivity areas. Comput. Geosci. 46, 272–283.

[6] Harris, J.R., Grunsky, E.C., 2015. Predictive lithological mapping of Canada's North using Random Forest classification applied to geophysical and geochemical data. Comput. Geosci. 80, 9–25.

[7] Yousefi, M., Carranza, E.J.M., 2015a. Fuzzification of continuous-value spatial evidence for mineral prospectivity mapping. Comput. Geosci. 74, 97–109.

[8] Yousefi, M., Carranza, E.J.M., 2015b. Prediction-area (P-A) plot and C-A fractal analysis to classify and evaluate evidential maps for mineral prospectivity modeling. Comput. Geosci. 79, 69–81.

[9] Yousefi, M., Carranza, E.J.M., 2015c. Geometric average of spatial evidence data layers: a GIS-based multi-criteria decision-making approach to mineral prospectivity mapping. Comput. Geosci. 83, 72–79.

[10] Yousefi, M., Carranza, E.J.M., 2016. Data-driven index overlay and Boolean logic mineral prospectivity modeling in greenfields exploration. Nat. Resour. Res. 25, 3–18.

[11] Ford, A., Miller, J.M., Mol, A.G., 2016. A comparative analysis of weights of evidence, evidential belief functions, and fuzzy logic for mineral potential mapping using incomplete data at the scale of investigation. Nat. Resour. Res. 25, 19–33.

[12] Yousefi, M., Nyk¨anen, V., 2017. Introduction to the special issue: GIS-based mineral potential targeting. J. Afr. Earth Sci. 12, 1–4.

[13] Abedi, M. 2018. An integrated approach to evaluate the Aji-Chai potash resources in Iran using potential field data. Journal of African Earth Sciences, 139, 379-391.

[14] Li, N., Song, X., Li, C., Xiao, K., Li, S., Chen, H., 2019. 3D geological modeling for mineral system approach to GIS-based prospectivity analysis: case study of an MVT Pb–Zn deposit. Nat. Resour. Res. 28 (3), 995–1019.

[15] Kreuzer, O. P., Yousefi, M., Nykänen, V. 2020. Introduction to the special issue on spatial modelling and analysis of ore-forming processes in mineral exploration targeting. Ore Geology Reviews, 119, 103391.

[16] Yousefi, M., Carranza, E. J. M., Kreuzer, O. P., Nykänen, V., Hronsky, J. M., Mihalasky, M. J. 2021. Data Analysis Methods for Prospectivity Modelling as applied to Mineral Exploration Targeting: State-of-the-Art and Outlook. Journal of Geochemical Exploration, 106839.

[17] Yousefi, M., Barak, S., Salimi, A., Yousefi, S. 2023a. Should Geochemical Indicators Be Integrated to Produce Enhanced Signatures of Mineral Deposits? A Discussion with Regard to Exploration Scale. Journal of Mining and Environment, 14(3), 1011-1018.

[18] Yousefi, M., Yousefi, S., Kamkar Rouhani, A. G. 2023b. Recognition coefficient of spatial geological features, an approach to facilitate criteria weighting for mineral exploration targeting. International Journal of Mining and Geo-Engineering.

[19] Ghasemzadeh, S., Maghsoudi, A., Yousefi, M., Mihalasky, M. J. 2022a. Information value-based geochemical anomaly modeling: A statistical index to generate enhanced geochemical signatures for mineral exploration targeting. Applied Geochemistry, 136, 105177.

[20] Yousefi, M., Hronsky, J. M. 2023. Translation of the function of hydrothermal mineralization-related focused fluid flux into a mappable exploration criterion for mineral exploration targeting. Applied Geochemistry, 149, 105561.

[21] Mostafaei, K., Kianpour, M.,Yousefi, M. 2023. Delineation of gold exploration targets based on the prospectivity models through an optimization algorithm. Journal of Mining and Environment, (), -. doi: 10.22044/jme.2023.13472.2489.

[22] Hronsky, J.M.A., Kreuzer, O.P., 2019. Applying spatial prospectivity mapping to exploration targeting: fundamental practical issues and suggested solutions for the future. Ore Geol. Rev. 107, 647–653.

[23] McCuaig, T.C., Hronsky, J.M.A., 2000. The current status and future of the interface between the exploration industry and economic geology research. Rev. Econ. Geol. 13, 553–559.

[24] Ford, A., McCuaig, T.C., 2010. The effect of map scale on geological complexity for computer-aided exploration targeting. Ore Geol. Rev. 38, 156–167.

[25] Joly, A., Porwal, A., McCuiag, T.C., 2012. Exploration targeting for orogenic gold deposits in the Granites-Tanami Orogen: mineral system analysis, targeting model and prospectivity analysis. Ore Geol. Rev. 48, 349–383.

[26] Hagemann, S.G., Lisitsin, V.A., Huston, D.L., 2016. Mineral system analysis: Quo vadis. Ore Geol. Rev. 76, 504–522.

[27] Yousefi, M., Kreuzer, O. P., Nykänen, V., Hronsky, J. M. 2019. Exploration information systems–A proposal for the future use of GIS in mineral exploration targeting. Ore Geology Reviews, 111, 103005.

[28] Ghasemzadeh, S., Maghsoudi, A., Yousefi, M., Mihalasky, M. J. 2022b. Recognition and incorporation of mineralization-efficient fault systems to produce a strengthened anisotropic geochemical singularity. Journal of Geochemical Exploration, 235, 106967.

[29] Bahri, E., Alimoradi, A., Yousefi, M. 2023. Investigating the performance of continuous weighting functions in the integration of exploration data for mineral potential modeling using artificial neural networks, geometric average and fuzzy gamma operators. International Journal of Mining and Geo-Engineering.

[30] Grunsky, E. C., de Caritat, P. 2020. State-of-the-art analysis of geochemical data for mineral exploration. Geochemistry: Exploration, Environment, Analysis, 20, 217-232.

[31] Pirajno, F. 2008. Hydrothermal processes and mineral systems. Springer Science & Business Media.

[32] Zuo, R., Zhang, Z., Zhang, D., Carranza, E.J.M., Wang, H., 2015. Evaluation of uncertainty in mineral prospectivity mapping due to missing evidence: a case study with skarntype Fe deposits in Southwestern Fujian Province, China. Ore Geol. Rev. 71, 502–515.

[33] Yousefi, M. 2017a. Recognition of an enhanced multi-element geochemical signature of porphyry copper deposits for vectoring into mineralized zones and delimiting exploration targets in Jiroft area, SE Iran. Ore Geology Reviews, 83, 200-214.

[34] Yousefi, M. 2017b. Analysis of zoning pattern of geochemical indicators for targeting of porphyry-Cu mineralization: a pixel-based mapping approach. Natural Resources Research, 26, 429-441.

[35] Afzal, P., Yousefi, M., Mirzaie, M., Ghadiri-Sufi, E., Ghasemzadeh, S., Daneshvar Saein, L. 2019. Delineation of podiform-type chromite mineralization using geochemical mineralization prospectivity index and staged factor analysis in Balvard area (SE Iran). Journal of Mining and Environment, 10, 705-715.

[36] Zuo, R., Xiong, Y., Wang, J., Carranza, E. J. M. 2019. Deep learning and its application in geochemical mapping. Earth-science reviews, 192, 1-14.

[37] Zuo, R., 2020. Geodata Science-based mineral prospectivity mapping: a review. Nat. Resour. Res. 29, 3415–3424.

[38] Yousefi, M., Kamkar-Rouhani, A., Carranza, E. J. M. 2012. Geochemical mineralization probability index (GMPI): a new approach to generate enhanced stream sediment geochemical evidential map for increasing probability of success in mineral potential mapping. Journal of Geochemical Exploration, 115, 24-35.

[39] Chen, J., Yousefi, M., Zhao, Y., Zhang, C., Zhang, S., Mao, Z., Peng, M., Han, R., 2019. Modelling ore-forming processes through a cosine similarity measure: Improved targeting of porphyry copper deposits in the Manzhouli belt, China. Ore Geology Reviews, 107, 108-118.

[40] Ghasemzadeh, S., Maghsoudi, A., Yousefi, M., Mihalasky, M. J. 2019a. Stream sediment geochemical data analysis for district-scale mineral exploration targeting: Measuring the performance of the spatial U-statistic and CA fractal modeling. Ore Geology Reviews, 113, 103115.

[41] Ghasemzadeh, S., Maghsoudi, A., Yousefi, M. 2019b. Application of geometric average approach for Cu-porphyry prospectivity mapping in the Baft area, kerman. Journal of Geoscience, 29, 231-130.

[42] Ghasemzadeh, S., Maghsoudi, A., Yousefi, M. 2021. Identifying porphyry-Cu geochemical footprints using local neighborhood statistics in Baft area, Iran. Frontiers of Earth Science,15, 106-120.

[43] Zuo, R. 2018. Selection of an elemental association related to mineralization using spatial analysis. Journal of Geochemical Exploration, 184, 150-157.

[47] Cheng, Q. 2007. Mapping singularities with stream sediment geochemical data for prediction of undiscovered mineral deposits in Gejiu, Yunnan Province, China. Ore Geology Reviews, 32, 314- 324.

[45] Xiao, F., Chen, J., Hou, W., Wang, Z., Zhou, Y., Erten, O. 2018. A spatially weighted singularity mapping method applied to identify epithermal Ag and Pb-Zn polymetallic mineralization associated geochemical anomaly in Northwest Zhejiang, China. Journal of Geochemical Exploration, 189, 122-137.

[46] Xiao, F., Wang, K., Hou, W., Erten, O. 2020. Identifying geochemical anomaly through spatially anisotropic singularity mapping: A case study from silver-gold deposit in Pangxidong district, SE China. Journal of Geochemical Exploration, 210, 106453.

[48] MamiKhalifani, F., Bahroudi, A., Aliyari, F., Abedi, M., Yousefi, M., Mohammadpour, M. 2019. Generation of an efficient structural evidence layer for mineral exploration targeting. Journal of African Earth Sciences, 160, 103609.

[49] Berman, M. 1977. Distance distributions associated with

Poisson processes of geometric figures. Journal of Applied Probability, 195-199.

[50] Breiman, L., 2001. Random Forests. Mach. Learn. 45, 5–32.

[51] Mohebi, A., Mirnejad, H., Lentz, D., Behzadi, M., Dolati, A., Kani, A., Taghizadeh, H. 2015. Controls on porphyry Cu mineralization around Hanza Mountain, south-east of Iran: An analysis of structural evolution from remote sensing, geophysical, geochemical and geological data. Ore Geology Reviews, 69, 187-198.

[52] Alimohammadi, M., Alirezaei, S., Kontak, D. J. 2015. Application of ASTER data for exploration of porphyry copper deposits: A case study of Daraloo–Sarmeshk area, southern part of the Kerman copper belt, Iran. Ore Geology Reviews, 70, 290-304.

[53] Zolanj, S., Dimitrijevic, M.N., Cvetic, S., Dimitrijevic, M.D., 1972. Geological Map of Sarduiyeh (1:100,000). Geological Survey of Iran publication.

[54] Zuo, R., Wang, J., Chen, G., Yang, M. 2015. Identification of weak anomalies: A multifractal perspective. Journal of Geochemical Exploration, 148, 12-24.

[55] Sillitoe, R. H., 2010., Porphyry copper systems. Econ. Geol.105,3–41.

[56] Almasi, A., Yousefi, M., Carranza, E.J.M., 2017. Prospectivity analysis of orogenic gold deposits in Saqez-Sardasht Goldfield, Zagros Orogen, Iran. Ore Geol. Rev. 91, 1066–1080.

[57] Yousefi, M., Nyk¨anen, V., 2016. Data-driven logistic-based weighting of geochemical and geological evidence layers in mineral prospectivity mapping. J. Geochem. Explor. 164, 94–106.

[58] McCuaig, T.C., Beresford, S., Hronsky, J., 2010. Translating the mineral systems approach into an effective exploration targeting system. Ore Geol. Rev. 38, 128–138.

[59] Kreuzer, O.P., Miller, A.V., Peters, K.J., Payne, C., Wildman, C., Partington, G.A., Puccioni, E., McMahon, M.E., Etheridge, M.A., 2015. Comparing prospectivity modelling results and past exploration data: a case study of porphyry Cu–Au mineral systems in the Macquarie Arc, Lachlan Fold Belt, New South Wales. Ore Geol. Rev. 71, 516–544.

[60] Cooke, D. R., Hollings, P., Wilkinson, J. J., Tosdal, R. M. 2014. Geochemistry of porphyry deposits.

[61] Byrne, K., Lesage, G., Morris, W.A., Enkin, R.J., Gleeson, S.A., Lee, R.G., 2019. Variability of outcrop magnetic susceptibility and its relationship to the porphyry Cu centers in the Highland Valley Copper district. Ore Geol. Rev. https://doi.org/10.1016/j.oregeorev.2019.02.015.

[62] Kreuzer, O.P., Etheridge, M.A., Guj, P., McMahon, M.E., Holden, D.J., 2008. Linking mineral deposit models to quantitative risk analysis and decision-making in exploration. Econ. Geol. 103, 829–850.

[63] Carranza, E. J. M., Laborte, A. G. 2015. Data-driven predictive mapping of gold prospectivity, Baguio district, Philippines: Application of Random Forests algorithm. Ore Geology Reviews, 71, 777-787.

[64] Carranza, E. J. M., Laborte, A. G. 2016. Data-driven predictive modeling of mineral prospectivity using random forests: a case study in Catanduanes Island (Philippines). Natural Resources Research, 25, 35-50.

[65] Yousefi, M., Carranza, E.J.M., 2017. Union score and fuzzy logic mineral prospectivity mapping using discretized and continuous spatial evidence values. J. Afr. Earth Sci. 128, 47–60.

[66] Abedi, M., Kashani, S. B. M., Norouzi, G. H., Yousefi, M. 2017. A deposit scale mineral prospectivity analysis: A comparison of various knowledge-driven approaches for porphyry copper targeting in Seridune, Iran. Journal of African Earth Sciences, 128, 127-146.

[67] Rodriguez-Galiano, V., Sanchez-Castillo, M., Chica-Olmo, M., Chica-Rivas, M. 2015. Machine learning redictive models for mineral prospectivity: An evaluation of neural networks, random forest, regression trees and support vector machines. Ore Geology Reviews, 71, 804-818.

[68] Belgiu, M., Drăguţ, L. 2016. Random forest in remote sensing: A review of applications and future directions. ISPRS Journal of Photogrammetry and Remote Sensing, 114, 24-31.

[69] Karimpouli, S., Salimi, A., Ghasemzadeh, S. 2016. Seminonlinear spectral unmixing using a neural network based forward modeling. Journal of Applied Remote Sensing, 10,036006.

[70] Rodriguez-Galiano, V. F., Chica-Olmo, M., Chica-Rivas, M. 2014. Predictive modelling of gold potential with the integration of multisource information based on random forest: a case study on the Rodalquilar area, Southern Spain. International Journal of Geographical Information Science, 28, 1336-1354.

[71] Chung, C. J. F., Fabbri, A. G. 2003. Validation of spatial prediction models for landslide hazard mapping. Natural Hazards, 30, 451-472.

[72] Nykänen, V., Lahti, I., Niiranen, T., Korhonen, K. 2015. Receiver operating characteristics (ROC) as validation tool for prospectivity models—A magmatic Ni–Cu case study from the Central Lapland Greenstone Belt, Northern Finland. Ore Geology Reviews, 71, 853-860.

[73] Nykänen, V., Niiranen, T., Molnár, F., Lahti, I., Korhonen, K., Cook, N., Skyttä, P. 2017. Optimizing a knowledge-driven prospectivity model for gold deposits within Peräpohja Belt, Northern Finland. Natural Resources Research, 26, 571-584.

[74] Robinson, G. R., Larkins, P. M. 2007. Probabilistic prediction models for aggregate quarry siting. Natural Resources Research, 16, 135-146.

[75] Nykänen, V. 2008. Radial basis functional link nets used as a prospectivity mapping tool for orogenic gold deposits within the Central Lapland Greenstone Belt, Northern Fennoscandian Shield. Natural Resources Research, 17, 29-48.

[76] Lord, D. 2001. Measuring exploration success: an alternative to the discovery-cost-per-ounce method of quantifying exploration effectiveness. SEG Newsl., 45, 10-16.

[77] Hronsky, J.M.A., Groves, D.I., 2008. Science of targeting: definition, strategies, targeting and performance measurement. Aust. J. Earth Sci. 55, 3–12.

[78] Chen, Y., Wu, W. 2016. A prospecting cost-benefit strategy for mineral potential mapping based on ROC curve analysis. Ore Geology Reviews, 74, 26-38.

[79] Zuo, R., Xiong, Y. 2020. Geodata science and geochemical mapping. Journal of Geochemical Exploration, 209, 106431.

[80] Carranza, E. J. M., Hale, M. 1997. A catchment basin approach to the analysis of reconnaissance geochemical-geological data from Albay Province, Philippines. Journal of Geochemical Exploration, 60,157-171.

[81] Yilmaz, H. 2007. Stream sediment geochemical exploration for

gold in the Kazdağ dome in the Biga Peninsula, western Turkey. Turkish Journal of Earth Sciences, 16, 33-55.

[82] Yousefi, M., Carranza, E. J. M., Kamkar-Rouhani, A. 2013. Weighted drainage catchment basin mapping of geochemical anomalies using stream sediment data for mineral potential modeling. Journal of Geochemical Exploration, 128, 88-96.

[83] Lin, X., Meng, G., Pan, H., Cheng, Z., Yao, W., Cheng, X. 2019. Continental-scale stream sediment geochemical mapping in southern China: An insight into surface processes and tectonic framework. Journal of Geochemical Exploration, 207, 106362.

[84] Wang, J., Zhou, Y., Xiao, F. 2020. Identification of multi-element geochemical anomalies using unsupervised machine learning algorithms: A case study from Ag–Pb–Zn deposits in north-western Zhejiang, China. Applied Geochemistry, 120, 104679.

[85] Govett, G. J. S. 1983. Handbook of exploration geochemistry. Statistics, 2, 3-437.

[86] Berger, B. R., Ayuso, R. A., Wynn, J. C., Seal, R. R. 2008. Preliminary model of porphyry copper deposits. US geological survey open-file report, 1321, 55.

[87] Zuo, R., Carranza, E. J. M. 2011. Support vector machine: a tool for mapping mineral prospectivity